analytical chemistry

pubs.acs.org/ac Article

Simple Colorimetric and Fluorescence Chemosensing Probe for Selective Detection of Sn^{2+} Ions in an Aqueous Solution: Evaluation of the Novel Sensing Mechanism and Its Bioimaging Applications

Palanisamy Ravichandiran, Vignesh Krishnamoorthi Kaliannagounder, Antony Paulraj Bella, Anna Boguszewska-Czubara, Maciej Masłyk, Cheol Sang Kim, Chan Hee Park, Princy Merlin Johnson, Byung-Hyun Park, Myung-Kwan Han, Ae Rhan Kim, and Dong Jin Yoo*

Cite This: https://dx.doi.org/10.1021/acs.analchem.0c03196 Read Online

ACCESS | Metrics & More | Article Recommendations | Supporting Information

ABSTRACT: An easily accessible colorimetric and fluorescence probe 4-((3-chloro-1,4-dioxo-1,4-dihydronaphthalen-2-yl)amino)-benzenesulfonamide (**4CBS**) was successfully developed for the selective and sensitive detection of Sn^{2+} in an aqueous solution. The sensing mechanism involves reduction of −C═O into −C−OH groups in **4CBS** upon the addition of Sn^{2+}, which initiates the fluorescence turn-on mode. A better linear relationship was achieved between fluorescence intensity and Sn^{2+} concentration in the range of 0−62.5 μM, with a detection limit (LOD) of 0.115 μM. The binding mechanism of **4CBS** for Sn^{2+} was confirmed by Fourier transform infrared analysis, NMR titrations, and mass (electrospray ionization) spectral analysis. Likewise, the proposed sensing mechanism was supported by quantum chemical calculations. Moreover, bioimaging studies demonstrated that the chemosensing probe **4CBS** is an effective fluorescent marker for the detection of Sn^{2+} in living cells and zebrafish. Significantly, **4CBS** was able to discriminate between Sn^{2+} in human cancer cells and Sn^{2+} in normal live cells.

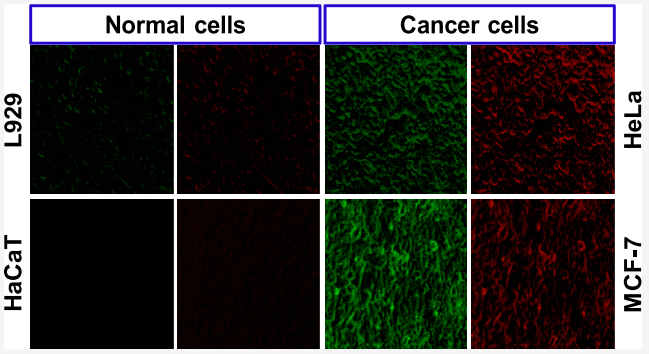

Industrialization has resulted in the release of a large amount of heavy metals into the environment, seriously threatening human life.[1−3] In the human body, small concentrations of inorganic cations take part in significant biological, chemical, and enzymatic activities at the cellular level.[4,5] However, excess consumption of these metal ions may lead to numerous neural disorders such as Wilson's disease, Alzheimer's disease, and Menkes syndrome.[6,7] Among the various transition metals, tin (Sn) is an important element in human health.[8] At trace levels, Sn(II) could help in the development of body muscles and act as an effective catalyst in the synthesis of nucleic acids and proteins. Tin also supports hair growth, maintains body homeostasis, and prohibits spread of cancer cells in humans.[9] A lack of Sn(II) can cause serious issues in humans such as loss of hearing, breathing trouble, and shortage of hemoglobin production.[10] However, accumulation of large amounts of Sn(II) can damage live cells, which would lead to inhibited zinc metabolism. This in turn can cause severe illness in both the lung and gastric systems.[11] Given the dangerous impacts of Sn(II) to humans, consumption of Sn(II) must be closely monitored. According to the World Health Organization's (WHO) guiding principles for metals, the maximum levels of allowed Sn(II) in drinking water and canned foods are 8.4×10^{-4} to 8.4×10^{-3} and 2.105×10^{-6} M, respectively.[12] Nevertheless, investigations on the physiological mechanisms associated with Sn(II) ions are limited because of the lack of effective Sn(II)-sensing methods. In the environmental perspective, Sn(II) can remain in the environment for a longer time and fairly remain non-biodegradable, while the accumulation of Sn(II) for several years on water soils distresses the microorganisms. Generally, Sn(II) can pollute the water system which induces the toxicity to algae, phytoplankton, and fungi.[13] Phytoplankton is an important microorganism which delivers oxygen to the other microorganisms in water. This is a significant measure of the food chain in the aquatic system. The surface of the water can be mainly polluted in contact with Sn(II) that inhibits the penetration of sunlight which pave the way of harmful effects to the aquatics life.[14] Besides, Sn(II) is the most dangerous divalent metal ion which induce several serious effects to the

Received: July 28, 2020
Accepted: November 26, 2020

https://dx.doi.org/10.1021/acs.analchem.0c03196
Anal. Chem. XXXX, XXX, XXX−XXX

humans. In recent times, Sn(II) is utilized in many fields such as paint/plastic industries and agricultural field via pesticides. The utilization of Sn(II) continuously increases, which is one of the major reasons for its poisoning. The Sn(II) has comparatively short hydrogen bonds, whereas humans can intake Sn(II) by breathing, by the consumption of food, and by the skin. The accumulation of Sn(II) can induce acute and long-term effects in the human body. The acute effects include eye irritations, heavy sweating, breathing trouble, and urination complications. The long-term effects are damage in liver functioning, disorders in the immune system, chromosomal destruction, damage in the brain, and lack of red blood cells.[15] Hence, Sn(II) is the most relevant and significant metal ion to study about its biological and environmental impacts. Besides, there is a significant need to develop simple and efficient methods for the detection of Sn(II) in the environment and biological bodies. This should provide precise, rapid, and highly sensitive responses to specific analytes.

Several analytical techniques have been reported for the detection and quantitative analysis of Sn ions. The determination of Sn^{2+} was reported using the atomic absorption spectroscopy in the aqueous solution with an LOD of 8.4×10^{-7} M.[16] Inductively coupled plasma mass spectroscopy was used for the sensing of Sn^{2+} and Sn^{4+} ions. The LOD for this study was achieved as 1.1×10^{-6} and 7.0×10^{-7} M, respectively.[17] Recently, UV/vis spectroscopy was employed in the identification of Sn^{2+} and the probe exhibits an LOD of 7.5×10^{-7} M.[18] X-ray fluorescence spectroscopy was used in the determination of Sn^{2+} in canned foods with an LOD of 4.2×10^{-5} M.[19] Also, a polymeric membrane-based ionophore was used to detect Sn^{2+} in real samples with an LOD of 4.0×10^{-6} M via potentiometric membrane detection techniques.[20] These methods have several practical disadvantages such as the need for expensive instruments/sophisticated maintenance, uncertain sample preparation, and the need for skilled operators. In contrast, optical recognition of analytes specifically for toxic materials is attracting wide attention among researchers in chemical, biological, and environmental analyses.[21] These optical sensors provide simple operation and have several practical advantages such as high selectivity/sensitivity, rapid response, inexpensive cost, real-time detection, and no need for sophisticated instruments. Among various optical sensors available today, fluorescence chemosensing probes have attracted wide attention and are recognized as a powerful tool for the detection of specific targets because of their simple operation, rapid response, and ability to bioimage live human or animal cells.[22] Colorimetric chemosensing probes have received much attention for metal ion detection because of their simple "naked-eye" recognition that can be easily monitored using simple spectroscopic instruments or even by an untrained technician. These combined colorimetric and fluorescence dual-channel chemosensing probes provide defined data with simple operative modes.[23] Typically, chemosensing probes consist of two major units, a receptor and a signal unit. Receptors such as amides, thiophenols, ureas, and pyrrole moieties are often used to bind with suitable metal ions, and molecules such as naphthoquinones function as a reporter for the detection of specific metal ions.[24] Naphthoquinone cores are widely present in many natural compounds such as lawsone, menadione, and plumbagin.[25] In our previous reports, we synthesized a new library of 1,4-naphthoquinones grafted with nitrogen and sulfur atoms and explored their anticancer,[26] cytotoxic,[27] and antibacterial[28] properties. It was established that nitrogen and sulfur atoms play a vital role to enhance the biological activities showed by the compounds. Also, naphthoquinone derivatives possess excellent fluorescent behavior, a good molar absorption coefficient, high quantum yield, and relatively low toxicity to normal human cells.[29] However, their utilization as chemical sensors for metal ions or biomolecule recognition is very limited. Hence, naphthoquinone backbones are suitable candidates for further development of selective chemosensing probes in the field of optical sensors.

Recently, some chemosensing probes were reported for the detection of Sn^{2+} ions. For example, Jonaghani et al. reported the synthesis of quinoline-based naphthothiazole as a fluorescent and colorimetric chemosensing probe for Zn^{2+} and Sn^{2+} ions.[30] Qu et al. described the preparation of carbazole-containing diarylethene units for the selective detection of Sn^{2+} and Cu^{2+} ions.[31] Very recently, Singh et al. reported the synthesis of N-heterocyclic unsymmetrical organosilatranes for the fluorescence detection of Sn^{2+} ions.[32] Salem et al. prepared citrate-stabilized silver nanoparticles for in situ sensing of Sn^{2+} ions.[10] Gao et al. described the synthesis of chiral carbon dot-based nanosensors for Sn^{2+} and lysine enantiomer recognition.[33] Recently, Gul et al. described the synthesis of phenolphthalein and BODIPY-based colorimetric/fluorescence dual-channel sensors for Sn^{2+} and Al^{3+} recognition and evaluated their bioimaging applications.[4] Most of these reported chemosensing probes have several practical disadvantages such as interference of coexisting metal ions, poor performance in aqueous solutions, poor selectivity, weak emission properties, and diminished biocompatibility which means that they induce the toxicity or immune response upon residing in the human/animal living cells. Thus, in the treatment of medical implants to the humans, the biocompatibility of the material is very important to avoid the denial of implantation by the body cells and tissues.[34]

The development of dual-channel fluorescence and colorimetric sensing probes for the detection of metal ions in the aqueous solutions is needed because of their color-based easy detection and need for inexpensive instruments. Specifically, dual-channel recognition of single-metal ion detection attracts wide attention because of the simple naked-eye detection, less time-consuming process, and highly efficient fluorescence analysis.[35] However, the maximum of the available dual-channel sensing probes are highly active in the organic medium, although these probes have shown weak sensing performance in the aqueous medium that restricts the applications in the environmental analysis. Besides, these probes are interfered with the same family of alkaline earth metal ions.[36] Hence, inspired by the requirement of active colorimetric/fluorescence chemosensing probes in the aqueous medium, we report the synthesis and sensing behavior of a new fluorescence and colorimetric chemosensing probe 4-((3-chloro-1,4-dioxo-1,4-dihydronaphthalen-2-yl)amino)-benzenesulfonamide (**4CBS**) that exhibited excellent selectivity and sensitivity toward Sn^{2+} in water (20 mM HEPES, pH = 7.5). The chemosensing probe displayed higher selectivity toward Sn^{2+}, whereas the interference of the coexisting metal ions was strictly inhibited. Moreover, the chemosensing probe **4CBS** presented a good limit of detection, complex stability constant (K_s), and rapid response (less than 10 s) in the aqueous medium than the formerly stated chemosensing probes.[31] Also, the sensor probe **4CBS** functioned through a novel sensing mechanism called reduction-enabled fluores-

https://dx.doi.org/10.1021/acs.analchem.0c03196
Anal. Chem. XXXX, XXX, XXX−XXX

Scheme 1. Green Synthesis of the Chemosensing Probe 4CBS in Water

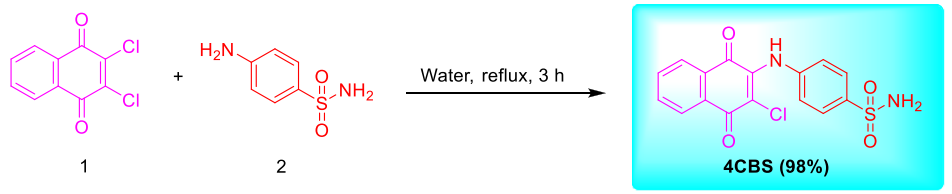

cence turn-on response which was thoroughly explored by Fourier transform infrared (FT-IR), NMR, and mass [electrospray ionization−mass spectrometry (ESI−MS)] spectral analyses. The detection of Sn^{2+} was accomplished in human live cells and zebrafish. Moreover, discriminative identification of Sn^{2+} in human cancer cells was demonstrated to prove the utility of the sensor probe **4CBS**. Moreover, very few sensing probes could discriminatively detect Sn^{2+} in human cancer cells from normal cells, and our reported chemosensing probe **4CBS** shows the best performances in terms of quick response (within 10 min) and the lower concentration of the ligand used.[30]

EXPERIMENTAL SECTION

Synthesis of the Ligand 4CBS. The ligand **4CBS** was synthesized according to our previously reported procedure with slight modifications (Scheme 1).[28] The procedure for the preparation of the ligand and its structural characterizations are briefly deliberated in the Supporting Information (Figures S1, S2).

Preparation of the Stock Solution. The stock solution of 2.0×10^{-3} M **4CBS** was prepared in 10 mL of dimethyl sulfoxide (DMSO) (0.0072 g). 1.0×10^{-1} M alkaline metal ions of Na^+, K^+, Cs^+, Li^+, Sr^{2+}, Ba^{2+}, Cd^{2+}, Zn^{2+}, Sn^{2+}, Ni^{2+}, Co^{2+}, Mg^{2+}, Ca^{2+}, Mn^{2+}, Hg^{2+}, Cu^{2+}, Fe^{2+}, Fe^{3+}, Al^{3+}, La^{3+}, and Sn^{4+} were prepared using double-distilled water. From the prepared stock solutions, 10 μL (2.50×10^{-4} M) of a metal ion solution and 25 μL of **4CBS** (1.25×10^{-5} M, predissolved in DMSO) were added into 3965 μL of the aqueous solution (20 mM HEPES, pH = 7.5). The proportion of the final 4000 μL of the prepared test solution contains 3975 μL of water and 25 μL of DMSO. The prepared solutions were used for metal ion-binding studies. Spectroscopic studies were carried out at room temperature (RT).

4CBS−Sn^{2+} Complex Preparation for Mass (ESI-MS) and FT-IR Analyses. An acetonitrile solution (CH_3CN, 15 mL) of the sensor probe **4CBS** (0.054 g, 0.01 M) and $SnCl_2$ (0.028 g, 0.01 M) was constantly stirred in the presence of trimethylamine (0.5 equiv) for 3 h at RT. The obtained solid complex was filtered and washed with anhydrous CH_3CN (40 mL). The isolated final product was characterized by FT-IR and ESI-MS analyses.

In Vitro Cytotoxicity Assay of 4CBS. Mouse fibroblast cells (L929), human keratinocyte cells (HaCaT), human cervical cancer cells (HeLa), and human breast cancer cells (MCF-7) were cultured in Dulbecco's modified Eagle medium (Hyclone, USA) at 37 °C with 5% CO_2. For cytotoxicity analysis, both cells were seeded with a density of 30,000 cells/well. After monolayer confluency, a cell culture media with 11 various concentrations of **4CBS** (0.0975−100 μM, predissolved in DMSO) was added to the respective wells. After 24 h treatment of **4CBS** with cells, a 10% CCK-8 solution (Dojindo Laboratories, Japan) was added to each well and incubated for 3 h. Later, the optical density was recorded at 450 nm (Microplate reader, Tecan, Austria). The cells without sample treatment were used as a control, and the cytotoxicity test was performed in triplicate.[37]

Live Cell Imaging Study. L929, HaCaT, HeLa, and MCF-7 cells were cultured in 24-well plates for 24 h for fluorescence bioimaging studies. Next, the culture media was removed and washed twice with 1× phosphate-buffered saline (PBS, pH = 7.4). The cells were treated with 6.25 μM Sn^{2+} for 10 min. After incubation, the cells were washed twice with PBS and treated with 6.25 μM **4CBS** for 10 min. Subsequently, the cells were washed thrice using PBS and fixed with paraformaldehyde (4%, Biosesang, Korea) solution for 5 min. Fluorescence images of the cells were captured using a fluorescence microscope (ECLIPSE Ts2-FL, Nikon) with 50 μm magnification under red and green filters. DIC images were captured under the white LED source. Fluorescence bioimaging studies were performed under a green filter (excitation = 488 nm; emission = 548 nm) and a red filter (excitation = 594 nm; emission = 654 nm). The mean fluorescence intensity of bioimages was determined using ImageJ software.[38]

Zebrafish Imaging Study. Hatched zebrafish babies were maintained in an E3 embryo medium (28 °C). At first, 6.25 μM Sn^{2+} (predissolved in water) was incubated with the zebrafish for 20 min. After the treatment period, the unreacted Sn^{2+} was removed by washing with PBS (pH = 7.4). Next, the metal-treated zebrafish were further incubated with 6.25 μM **4CBS** for 30 min. Finally, the unreacted traces of **4CBS** were removed by washing with PBS, and fluorescence bioimaging of zebrafish was conducted using a confocal laser scanning microscope (Carl Zeiss, Germany, LSM 510 META) under a green filter (excitation = 550 nm; emission = 580 nm) and red filter (excitation = 630 nm; emission = 660 nm) installed at the Center for University-Wide Research Facilities (CURF) at Jeonbuk National University (JBNU, Jeonju, South Korea).[38]

RESULTS AND DISCUSSION

Design and Synthesis of the Ligand 4CBS. The reducing and electrophilic properties are the most significant characters of the Sn^{2+} ion. From our previous report, it was found that the Sn^{2+} ion binds with the host molecule, the strong electronegative −OH or −NH groups preferably participating in the coordination mechanism.[39] Nevertheless, if the host molecule does not have −OH groups, the available redox centers (−C═O) in the host molecule can be reduced to −C−OH groups by the metal Sn^{2+} that enables the metal to bind. With respect to these features of Sn^{2+}, we rationally designed and synthesized the chemosensing probe **4CBS** which consists of strong electronegative groups (−NH) and reactive redox centers (−C═O) for the detection of the Sn^{2+} ion. The synthesis of the chemosensing probe **4CBS** was achieved by a simple, green approach, as presented in Scheme 1. The reaction of 2,3-dichloro-1,4-naphthoquinone (**1**) with

https://dx.doi.org/10.1021/acs.analchem.0c03196
Anal. Chem. XXXX, XXX, XXX−XXX

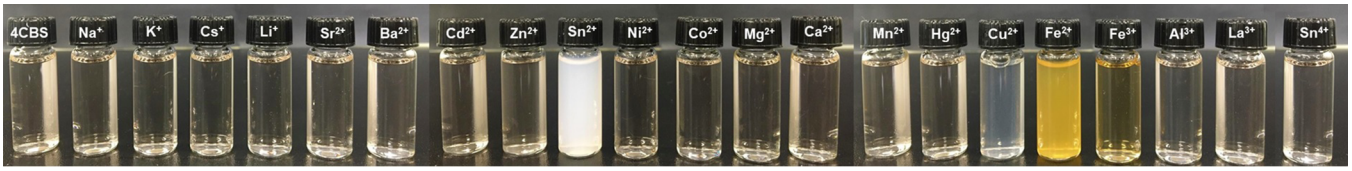

Figure 1. Visual recognition of metal ions (1.25×10^{-3} M) with the sensor probe **4CBS** (1.25×10^{-5} M) in the aqueous medium (20 mM HEPES, pH = 7.5).

p-aminobenzenesulfonamide (**2**) was carried out via a Michael-like addition reaction. The reaction was completed by a green method in which water was employed as a solvent medium. The nucleophilic substitution product of the ligand **4CBS** was obtained under reflux conditions for 3 h with an excellent yield.

Colorimetric Responses of 4CBS toward Metal Ions. In the beginning of the investigation, the colorimetric behavior of the sensor probe **4CBS** was evaluated upon the addition of 100 equiv of various alkaline earth metals in the aqueous medium (20 mM HEPES, pH = 7.5). As depicted in Figure 1, the light maroon color of the probe turned to milky white with the addition of Sn^{2+}. The prepared chemosensing probe **4CBS** did not show any notable color changes with the addition of other metal ions. Poor yellow color conversions of Fe^{2+} and Fe^{3+} ions were noticed, but this was due to the original color of the iron ions.[40] The specific color change of **4CBS** with Sn^{2+} was attributed to the several electron transitions in the **4CBS**−Sn^{2+} complex such as π to π^*, d−d, ligand−metal charge-transfer, and metal−ligand charge-transfer effects.[41]

Emission Properties of 4CBS with Metal Ions. A solvatochromic study was carried out to determine the absorption behavior of the sensor probe **4CBS** in different solvents with 20 mM HEPES, pH = 7.5. The obtained absorption spectrum showed three strong peaks for **4CBS** at 233, 280, and 467 nm. The examined absorption behavior of **4CBS** in different solvents and water displayed a smooth UV/vis spectrum with high ligand solubility (Figure S3). Water with 20 mM HEPES, pH = 7.5 was selected for metal ion-binding studies because of the excellent performance of the ligand **4CBS** in the aqueous medium. Also, a wavelength of 280 nm was carefully chosen as the fluorescence excitation wavelength based on the fluorescence study of **4CBS** at different excitation wavelengths (Figure S4). In contrast, using a lower excitation wavelength for highly diluted solutions shows a fine emission spectrum.[42] However, employing such a lower excitation wavelength associated with other practical challenges is likely harmful to the skin/eyes to the humans and besides, it leads to the DNA damage in tissues of the biological system. Thus, extensive care must be taken while employing such a lower excitation system for the environmental and biological sample analysis.[43] Initially, selectivity of the sensor probe was determined with 20 various metal ions (2.50×10^{-4} M) of Na^+, K^+, Cs^+, Li^+, Sr^{2+}, Ba^{2+}, Cd^{2+}, Zn^{2+}, Ni^{2+}, Co^{2+}, Mg^{2+}, Ca^{2+}, Mn^{2+}, Hg^{2+}, Cu^{2+}, Fe^{2+}, Fe^{3+}, Al^{3+}, La^{3+}, and Sn^{4+}. No obvious fluorescence improvement was obtained in the emission spectrum of **4CBS** (1.25×10^{-5} M). Upon the addition of Sn^{2+} (2.50×10^{-4} M) to the **4CBS** solution, the intensity of the emission peak was significantly increased via the fluorescence turn-on mode. Adding Sn^{2+} to the aqueous solution of **4CBS** resulted in a 43-fold higher emission intensity than that of the ligand **4CBS** alone because of exciplex complex formation (Figure 2). According to the colorimetric responses of the ligand **4CBS** toward Sn^{2+}, it is clearly shown that the ligand was formed the aggregated

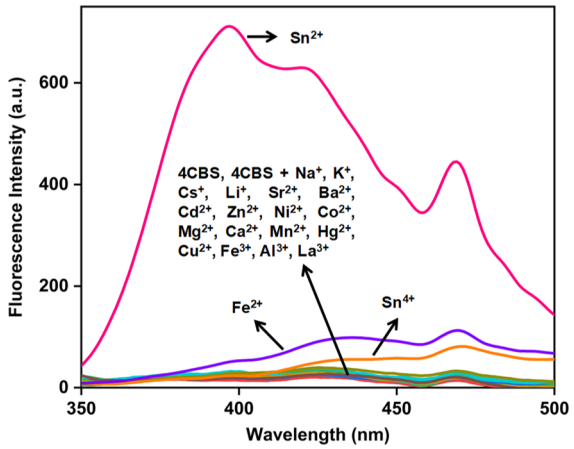

Figure 2. Fluorescence selectivity study of **4CBS** in the presence and absence of various M^{n+} in the aqueous solution; λ_{ex} = 280 nm.

particles with Sn^{2+} in water. To characterize this aggregation phenomenon, initially, the dynamic light scattering (DLS) analysis was carried out to confirm the intriguing **4CBS**−Sn^{2+} aggregation. The DLS analysis of the **4CBS**−Sn^{2+} complex indicates the maximum particle size distribution obtained at 190.50 ± 18.52 nm with 5.0×10^{-4} M Sn^{2+}. However, the population of aggregated particles was reduced upon the addition of higher concentration of 1.25×10^{-3} M Sn^{2+} (164.22 ± 12.30 nm, Figures S5, S6). To get a deep insight into the formation of aggregated particles, the morphology of the **4CBS**−Sn^{2+} complex was studied by atomic force microscopy. The obtained results indicate that the particle size distribution is more consistent to the DLS analysis of the **4CBS**−Sn^{2+} complex (Figures S7, S8). Besides, the effect of aggregates/precipitates in the fluorescence emission property of the **4CBS**−Sn^{2+} complex was explored. Upon the addition of increased concentration of Sn^{2+} (0−100 equiv) to the aqueous **4CBS** solution, without any intervention, the fluorescence emission intensity was progressively intensified up to 60 equiv of Sn^{2+}, although small/acceptable emission decrement was noticed with the addition of 70−100 equiv of Sn^{2+} to the aqueous **4CBS** that was due to the formation of larger aggregated particles. These combined results indicate that the formed aggregates/precipitates induced negligible effects in the emission intensity for the **4CBS**−Sn^{2+} complex in the aqueous solution (Figure S9). The fluorescence changes of the **4CBS**−Sn^{2+} complex in an aqueous environment were explored by the addition of different amounts of CH_3CN. The fluorescence intensity of the **4CBS**−Sn^{2+} complex increased in 80−100% aqueous medium (Figure S10). Moreover, the concentration of the HEPES, pH = 7.5 buffer for the **4CBS**−Sn^{2+} complex was investigated, and a 20 mM HEPES, pH = 7.5 buffer solution was sufficient to show the higher fluorescence intensity (Figure S11). The solvent effect was also studied for the **4CBS**−Sn^{2+} complex, and none of the organic solvents

https://dx.doi.org/10.1021/acs.analchem.0c03196
Anal. Chem. XXXX, XXX, XXX−XXX

increased the emission intensity. Nevertheless, higher fluorescence intensity was observed in water than in other solvents (Figure S12). Therefore, water with 20 mM HEPES, pH = 7.5 (which contains 99.375:0.625 v/v of H_2O/DMSO) buffer was used as an optimized solvent medium for **4CBS** to recognize Sn^{2+}.

After we determined the selectivity of **4CBS** for Sn^{2+}, quantitative analysis of Sn^{2+} was carried out in the aqueous solution (20 mM HEPES, pH = 7.5). As in Figure 3, an

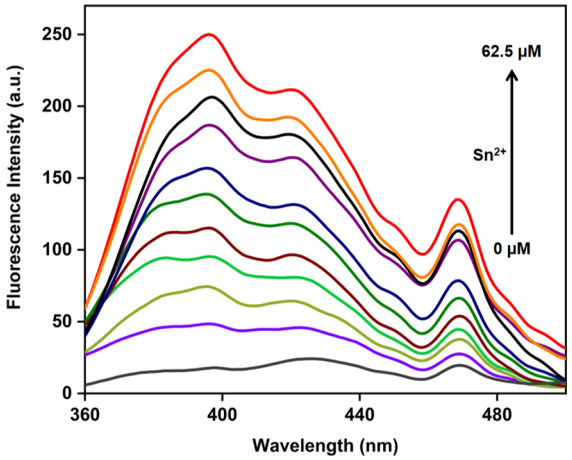

Figure 3. Emission titration analysis of **4CBS** (1.25×10^{-5} M) with the increased concentration of Sn^{2+} ($0-6.25 \times 10^{-5}$ M) in the aqueous solution (20 mM HEPES, pH = 7.5); λ_{ex} = 280 nm.

increase in the concentration of Sn^{2+} in the **4CBS** solution resulted in a gradual increase in the fluorescence emission band centered at 397 nm. A good linear relationship between fluorescence emission intensity and Sn^{2+} concentration was obtained in the range of 0−62.5 μM (R^2 = 0.9979, Figure S13). Thus, the fluorescence titration study indicates that the chemosensing probe **4CBS** has good detectability and could be used to quantitatively recognize Sn^{2+} in the aqueous medium. Next, we examined the effect of interference of other metal ions with the sensor probe **4CBS** and Sn^{2+}. In this study, various metal ions were added to the aqueous **4CBS**−Sn^{2+} complex (20 mM HEPES, pH = 7.5), and their fluorescence changes were recorded. The obtained results reveal that the coexistence of metal ions has no or a negligible influence on the sensing of Sn^{2+} by the probe **4CBS** (Figure 4). Moreover, the selectivity of **4CBS** was examined as the ratio of the slope of the calibration plot for Sn^{2+} to the slope of the plot for a given metal cation interference (Figure S14). Besides, the metal ion interference was examined by UV/vis complexometric titration analysis (Figure S15). These cumulative UV/vis and fluorescence studies recommend that the sensing property of the probe **4CBS** for Sn^{2+} was not influenced by the coexisting metal ions except Hg^{2+}, Fe^{2+}, and Fe^{3+} ions. The binding and the interference of these three metals were reduced to a significant amount of absorbance and fluorescence intensities; nevertheless, the obtained signals are still discernible to identify the presence of Sn^{2+}.

Evaluation of Coordination Stoichiometry and Complex Stability Constant. To evaluate the coordination ratio of the **4CBS**−Sn^{2+} system, we constructed a Job's plot.[44] As Sn^{2+} was added to the **4CBS** solution, the fluorescence intensity steadily increased. The highest emission intensity was obtained at a 0.5 mol fraction, which indicates a 1:1 binding

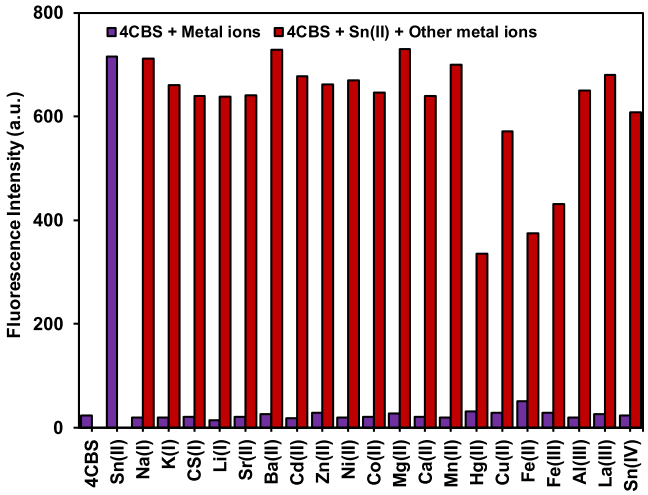

Figure 4. Complexometric titration of **4CBS** (1.25×10^{-5} M) and Sn^{2+} (2.50×10^{-4} M) with the coexistence of other metal ions (2.50×10^{-4} M) in the aqueous solution (20 mM HEPES, pH = 7.5); λ_{ex} = 280 nm; λ_{em} = 397 nm.

stoichiometric ratio attained in the **4CBS**−Sn^{2+} complex (Figure S16). Furthermore, the 1:1 binding ratio was confirmed by mass (ESI) analysis of the **4CBS**−Sn^{2+} complex (Figure S17). The peak for the sensor probe **4CBS** was obtained at a m/z of 363.00000 $[M]^+$ (calcd m/z 362.78400), and the peak for the **4CBS**−Sn^{2+} complex was noted at a m/z of 484.21024 $[M + Na]^+$ (calcd m/z 483.50890). This observation confirmed that the 1:1 binding ratio was obtained in the **4CBS**−Sn^{2+} complex. Next, the complex stability constant (K_s) was determined from the Benesi−Hildebrand analysis by employing the fluorescence titration data from Figure 3. The calculated K_s value was 5.0×10^6 M^{-1} (Figure S18). The detection limit (LOD) was calculated according to the formula $3\sigma/k$.[45] The calculated LOD value for Sn^{2+} detection was 0.115 μM, which is much lower compared to the WHO limitations.[46]

Reversibility Analysis of the Ligand 4CBS. Reversibility is a requirement in the development of novel chemical sensors in real-time applications. Thus, the reversibility behavior of **4CBS** was investigated with the added amount of Sn^{2+}. The fluorescence intensity increased after adding a certain amount of Sn^{2+} to the aqueous **4CBS** (20 mM HEPES, pH = 7.5). This fluorescence intensity diminished after the addition of a chelating agent ethylenediaminetetraacetic acid (EDTA) (140 equiv) into the **4CBS**−Sn^{2+} complex. Furthermore, the reversibility competence of the chemosensing probe **4CBS** was analyzed. The obtained results show that the chemosensing probe **4CBS** could be reversed by a maximum of 3 cycles (Figure S19). These findings reveal that the chemosensing probe **4CBS** was regenerated, supporting the high-grade reversibility of **4CBS** (Figure 5).

Evaluation of the Binding Mechanism. *FT-IR Analysis.* To explore the obtained sensing mechanism, we performed FT-IR analysis of the **4CBS**−Sn^{2+} complex. As given in Figure 6, the vibrational frequencies of the functional groups in the sensor probe **4CBS** were identified. Very strong and sharp signals were obtained for −NH (3346 cm^{-1}) and $-NH_2$ (3216 cm^{-1}) groups. After establishing coordination bonds of **4CBS** with Sn^{2+}, a red-shifted IR signal appeared for the −NH group (3349 cm^{-1}), whereas no peak shift was noticed for the $-NH_2$ group (3216 cm^{-1}). Moreover, a strong new stretching

https://dx.doi.org/10.1021/acs.analchem.0c03196
Anal. Chem. XXXX, XXX, XXX−XXX

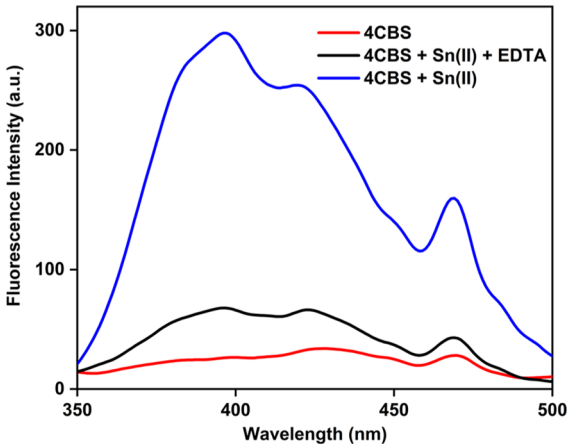

Figure 5. Ligand regenerative study of **4CBS** (1.25×10^{-5} M) with the addition of Sn^{2+} (6.25×10^{-5} M) and EDTA (1.75×10^{-3} M) in the aqueous solution (20 mM HEPES, pH = 7.5); λ_{ex} = 280 nm.

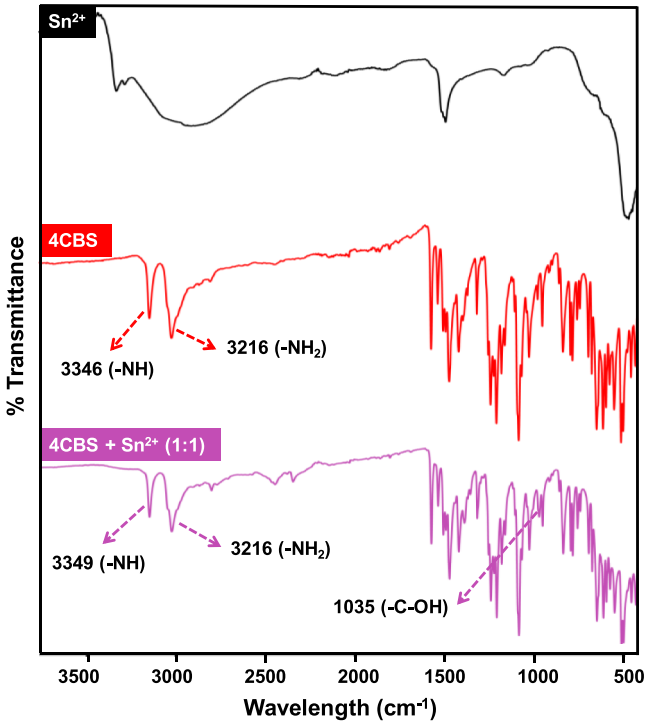

Figure 6. FT-IR analysis of $SnCl_2$, **4CBS**, and **4CBS**−Sn^{2+} complex.

vibration signal appeared for the −C−OH group at 1035 cm^{-1} because of the reduction of −C═O groups in the naphthoquinone moiety. IR signals showed negligible or no changes for the remaining aromatic functional groups in **4CBS**. This binding mechanism can be rationally explained in the following ways. It is known that the metal ion Sn^{2+} is a strong reducing agent, which can easily reduce ketonic group into alcohols. Hence, it reduced −C═O to −C−OH in the naphthoquinone core. According to Pearson's principle for acid−base theory, strong electronegative functional groups such as −OH and −NH in **4CBS** were strongly attracted to the strong electrophilic borderline base Sn^{2+}.[47] Therefore, the obtained results indicate that coordination bonding of **4BCS** and Sn^{2+} occurred by a reduction-enabled detection pathway in which −OH and −NH groups were involved in the bonding mechanism.

NMR Titration Analysis. After receiving the basic information about the coordination mechanism in the **4CBS**−Sn^{2+} complex, NMR titration studies were performed to acquire direct evidence for functional group participation in the coordination mechanism. ^{1}H NMR analysis of **4CBS** was carried out with an increasing amount of Sn^{2+}. As shown in Figure 7, the peak at 9.4799 ppm belongs to the −NH group in **4CBS**. As the concentration of Sn^{2+} in the **4CBS** solution increased, all the proton signals started to migrate in large upfield shifts. New signals for two −OH and one −NH groups appeared at 8.0077, 9.1782, and 9.3266 ppm, respectively. The intensity of −OH (9.1782 ppm) and −NH (9.3266 ppm) signals progressively decreased with increasing quantity of Sn^{2+}. All the proton signals were shifted (upfield) with the addition of 2 equiv of Sn^{2+}, and no further peak shifting was observed with excess Sn^{2+}, indicating that the sensor probe **4CBS** reached its maximum saturation level at the solution state.

Then, ^{13}C NMR analysis was investigated to confirm the reduction reaction-enabled sensing mechanism of the probe **4CBS**. Strong signals for −C═O groups in the naphthoquinone moiety were obtained at 176.9433 and 179.9464 ppm. The highest upfield shifts of all the carbon signals were observed upon adding 2 equiv of Sn^{2+}. Specifically, the carbon signals for −C−OH groups in the reduced form of **4CBS** were found at 141.7613 and 143.5276 ppm (Figure 8). After ^{13}C NMR titration analysis, distortionless enhancement by polarization transfer (DEPT) NMR analysis was carried out to determine if any of the aromatic rings that participated in the reduction reaction was induced by Sn^{2+}. Eight tertiary carbons are present in the chemosensing probe **4CBS**. When DEPT 90 and DEPT 135 NMR titration experiments were executed with 2 equiv of Sn^{2+} in the **4CBS** solution, signals for eight tertiary carbons with upfield shifting were found in both experiments. These combined results indicate that the aromatic rings were not influenced by the addition of Sn^{2+}, and the reduction reaction is more specific at −C═O centers (Figure 9). Consequently, the achieved cumulative NMR titration analyses revealed that a reduction-promoted sensing mechanism takes place between **4CBS** and Sn^{2+}. In addition, −NH and −OH functional groups in **4CBS** helped to establish the coordination bonding with Sn^{2+}.

*Electrochemical Investigation of the **4CBS**−Sn^{2+} Complex.* To gain a deeper insight into the sensing behavior of **4CBS** toward Sn^{2+}, an electrochemical investigation was accomplished using the cyclic voltammetry technique. First, the electrochemical properties of **4CBS** were measured in a CH_3CN solution of 0.1 M tetrabutylammonium tetrafluoroborate (supporting electrolyte) at a scan rate of 0.1 V s^{-1}. The sensor probe **4CBS** showed distinctive reduction peaks at −1.517 and −1.121 V and oxidation peaks at −1.231 and −1.651 V. As Sn^{2+} was added to the **4CBS** medium, the peak current for the **4CBS**−Sn^{2+} complex significantly increased with large potential shifts at −0.944 and −1.310 V (Figure S20). These results indicate that the chemosensing probe **4CBS** has strong affinity and sensitivity toward Sn^{2+}.

Theoretical Calculations. Theoretical calculations were executed for **4CBS** and **4CBS**−Sn^{2+} complex systems using the Gaussian 16 package. In the optimized structure of **4CBS**, the positions of naphthoquinone and sulfonamide units were nearly in the same plane. The optimized structure of the **4CBS**−Sn^{2+} complex showed the formation of hydrogen bonds of Sn^{2+} with −OH and −NH groups in the naphthoquinone

https://dx.doi.org/10.1021/acs.analchem.0c03196
Anal. Chem. XXXX, XXX, XXX−XXX

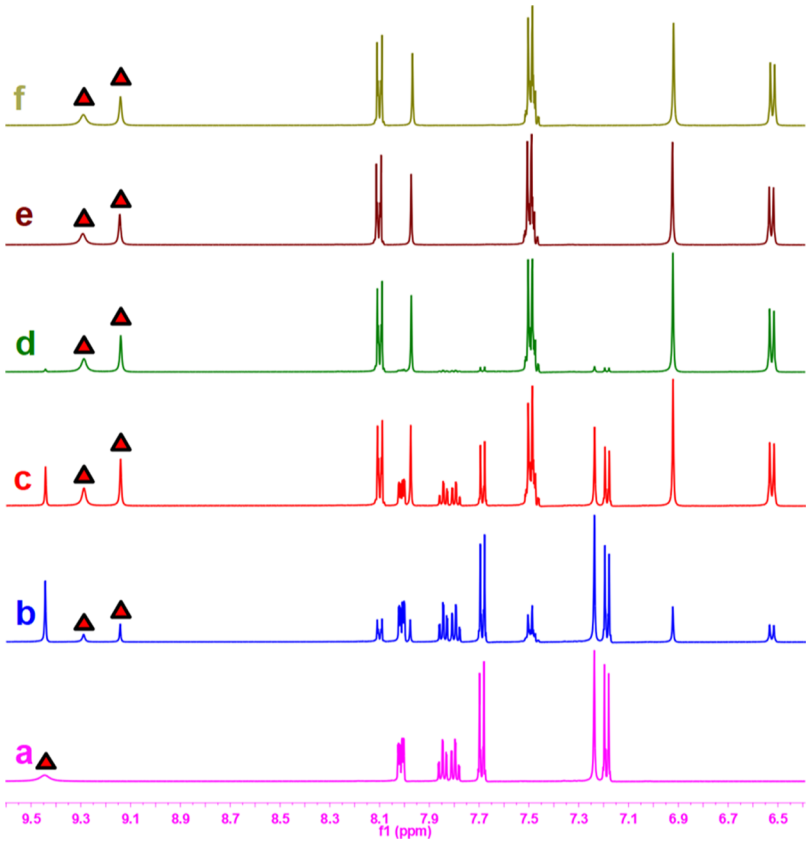

Figure 7. ^{1}H NMR titration study of **4CBS** (3.0×10^{-2} M, 0.0054 g) with (a) 0.0, (b) 0.5, (c) 1.0, (d) 1.5, (e) 2.0, and (f) 2.5 equiv of Sn^{2+} in 0.5 mL of DMSO-d_6 (with 20 mM HEPES, pH = 7.5).

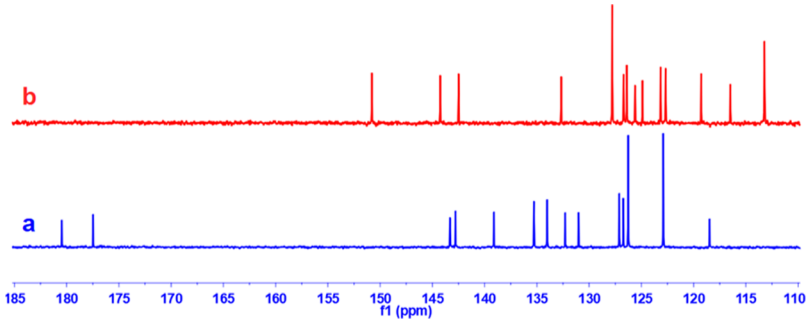

Figure 8. ^{13}C NMR titration study of **4CBS** (9.0×10^{-2} M, 0.0162 g) with (a) 0.0 and (b) 2.0 equiv of Sn^{2+} in 0.5 mL of DMSO-d_6.

unit, which enhanced the stability of the system (Figure S21). Next, the energy distributions of the highest occupied molecular orbital (HOMO) and lowest unoccupied molecular orbital (LUMO) energy levels for **4CBS** and its Sn^{2+} complex were examined. As shown in Figure 10, the energy of the HOMO and LUMO orbital levels for the **4CBS**−Sn^{2+} complex was lower than that of the ligand **4CBS**. Also, the energy differences of **4CBS** and **4CBS**−Sn^{2+} complex were calculated with an energy difference of 1.86 eV. These outcomes indicate that the effective resonance attraction obtained in the **4CBS**−Sn^{2+} complex. For the ligand **4CBS**, the energy migrated from the naphthoquinone unit to sulfonamide units because of the weak intramolecular charge-transfer (ICT) effect, whereas in the **4CBS**−Sn^{2+} complex, the maximum energy was localized at the naphthoquinone−Sn^{2+} units via a coordination bond caused by a strong ICT effect.[48] Hence, the obtained results imply that a stable complex was formed through the strong ICT effect, which is consistent with the proposed binding mechanism. The anticipated coordination mechanism of the **4CBS**−Sn^{2+} complex is given in Scheme 2.

Fluorescence Bioimaging Studies. *Identification of Sn^{2+} in Live Cells.* Encouraged by the outstanding photophysical properties of the ligand **4CBS** toward Sn^{2+}, its biocompatibility was investigated to detect Sn^{2+} in L929, HaCaT, HeLa, and MCF-7 cells using fluorescence bioimaging studies. First, the toxicity of the ligand **4CBS** was studied at 11 concentrations from 0.0975 to 100 μM. From the results, about 95% of the cells were viable to the sensor probe **4CBS**. However, the viability of the cells was reduced when **4CBS** was overdosed at concentrations of 25−100 μM (Figure S22). Therefore, the obtained results suggest that the ligand **4CBS** is biologically compatible and has low toxicity to live cells.

After the toxicity analysis of **4CBS**, a bioimaging study was carried out in L929, HaCaT, HeLa, and MCF-7 cells to

https://dx.doi.org/10.1021/acs.analchem.0c03196
Anal. Chem. XXXX, XXX, XXX−XXX

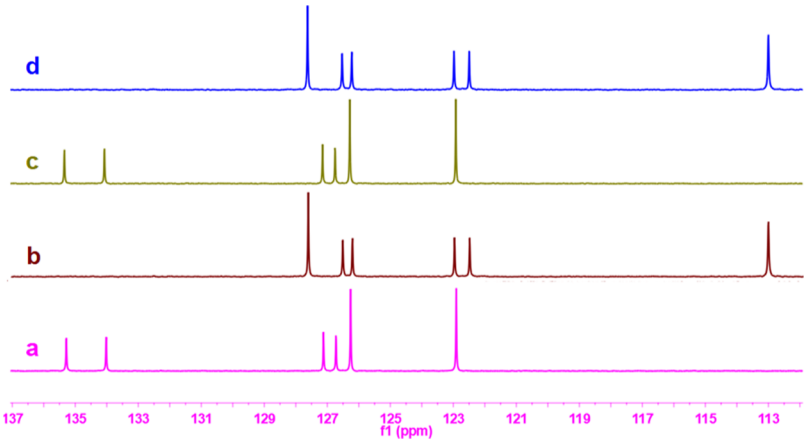

Figure 9. DEPT titration analysis of **4CBS** (9.0×10^{-2} M, 0.0162 g) in 0.5 mL of DMSO-d_6 (a) DEPT 90 analysis of **4CBS** without Sn^{2+}, (b) DEPT 90 analysis of **4CBS** with 2 equiv of Sn^{2+}, (c) DEPT 135 analysis of **4CBS** without Sn^{2+}, and (d) DEPT 135 analysis of **4CBS** with 2 equiv of Sn^{2+}.

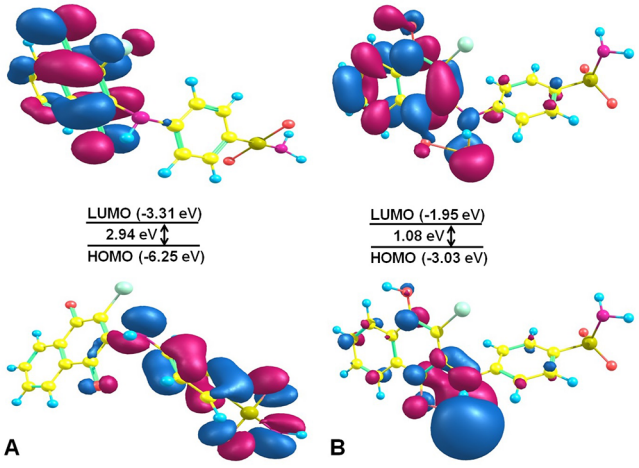

Figure 10. Theoretical calculations of the ligand **4CBS** (A) and **4CBS**–Sn^{2+} (B) complex.

Scheme 2. Proposed Detection Mechanism of the 4CBS–Sn^{2+} Complex

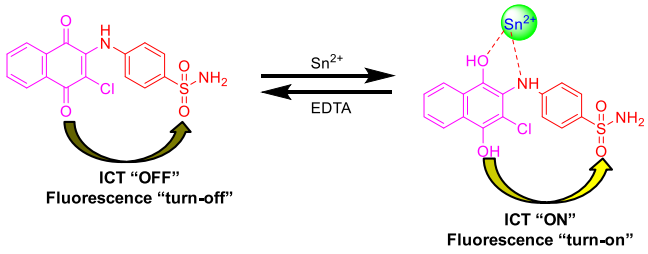

confirm the detection of Sn^{2+} in mouse fibroblast cells, human keratinocyte cells, human cervical cancer cells, and human breast cancer cells, respectively. Based on the toxicity study, two major concentrations of **4CBS** such as 6.125 and 12.50 μM were chosen for bioimaging analysis. Initially, 6.125 μM Sn^{2+} and **4CBS** were separately incubated with L929, HaCaT, HeLa, and MCF-7 cells for 10 min. A very weak/negligible level of fluorescence emission was observed in all the cells (Figures S23–S26). Next, 6.125 μM Sn^{2+} and **4CBS** were incubated in a combined manner with L929, HaCaT, HeLa, and MCF-7 cells for 10 min. As depicted in Figure 11, insignificant fluorescence emission was obtained for the ligand **4CBS** in L929 and HaCaT cells. Fascinatingly, robust fluorescence emission was induced by **4CBS** in HeLa and MCF-7 cells. Increased fluorescence intensities were obtained in HeLa and MCF-7 cells, compared to the fluorescence emission induced in L929 and HaCaT cells. The fluorescence intensity of HeLa and MCF-7 cells was increased in a dose-dependent manner (Figures S27–S30). In contrast, HeLa cells exhibit better fluorescence images than the MCF-7 cells (Figure S31). Furthermore, it can be noticed that the subcellular localization of **4CBS** made Sn^{2+} to mostly distribute in the cytoplasm of the cancer cells within 10 min. Thus, these results indicate that the sensor probe **4CBS** could easily penetrate the cancer cells (HeLa and MCF-7) and enhance the fluorescence emission intensity compared to normal live cells (L929 and HaCaT). The comparison of recently reported chemosensing probes with **4CBS** showing the K_s, LOD, and other analytical parameters is given in Table S1. In contrast, the sensing probe **4CBS** showed better sensitivity and selectivity toward Sn^{2+}. The bioimaging incubation period was competitively less than the reported sensing probes. Moreover, the ligand **4CBS** is well-performing in the aqueous medium through the colorimetric/fluorometric responses. In summary, the sensor probe **4CBS** may be capable of differentiating human cancer cells from the normal ones with high sensitivity/selectivity, and it has the potential to be utilized as an active bioimaging agent in biological analyses.

Bioimaging Studies in Zebrafish. Zebrafish larvae (5-day-old) were grown under optimal conditions in the E3 medium at 28 °C. Before adding the metal and ligand, the baby zebrafish were anaesthetized (50 mg/L tricaine). First, 6.125 μM Sn^{2+} was incubated alone with the zebrafish, and no or negligible fluorescence was emitted. Similar emission responses were perceived for incubation of the ligand **4CBS** (Figure 12a–f). Under a combined incubation of Sn^{2+} and **4CBS** (6.125 μM each), respectively, with the zebrafish, remarkable fluorescence intensity was detected around the eyes/yolk extension in both green and red filters (Figure 12g–i). The obtained data indicate that the chemosensing probe **4CBS** has tissue-penetrable capacity and is able to detect Sn^{2+} in small animals such as zebrafish.

https://dx.doi.org/10.1021/acs.analchem.0c03196
Anal. Chem. XXXX, XXX, XXX–XXX

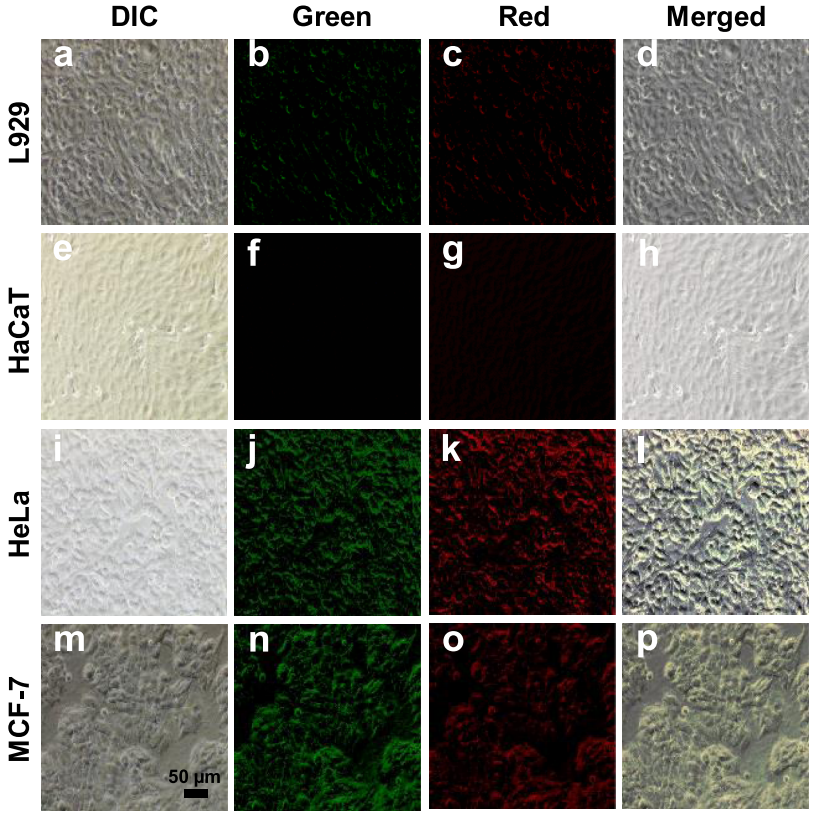

Figure 11. Fluorescence bioimaging detection of Sn^{2+} in L929, HaCaT, HeLa, and MCF-7 cells that are treated with 6.125 μM Sn^{2+} and **4CBS**, respectively, where images (a−d) = L929 cells; images (e−h) = HaCaT cells; images (i−l) = HeLa cells; and images (m−p) = MCF-7 cells.

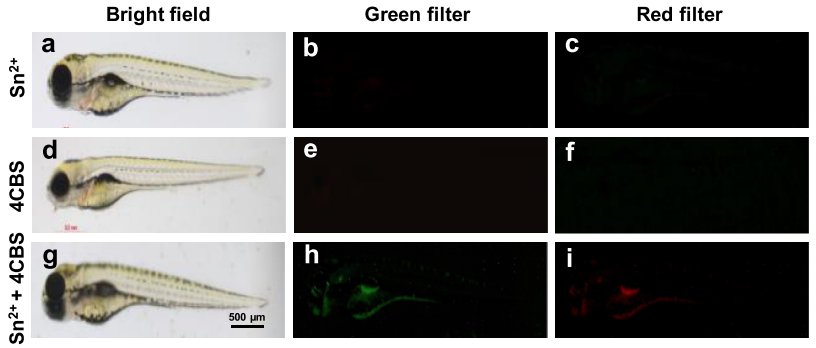

Figure 12. Confocal bioimaging of Sn^{2+} in zebrafish, where images (a−c) = zebrafish treated with 6.125 μM Sn^{2+}; images (d−f) = zebrafish treated with 6.125 μM **4CBS**; and images (g−i) = zebrafish treated with 6.125 μM Sn^{2+} and **4CBS**, respectively.

CONCLUSIONS

In conclusion, a new naphthoquinone-based colorimetric and fluorescence probe **4CBS** was successfully fabricated for recognition of Sn^{2+} in the aqueous medium under physiological pH. The structure of the synthesized chemosensing probe **4CBS** was analyzed by FT-IR, ^{1}H NMR, ^{13}C NMR, mass (ESI−MS), and elemental analyses. The sensing mechanism was triggered by the reduction of −C═O groups by Sn^{2+}, which was confirmed by spectroscopic investigations. Theoretical calculations were performed to justify the binding mechanism and optical behavior of the sensor probe. The chemosensing probe **4CBS** showed high selectivity and sensitivity for Sn^{2+} even in the presence of other metal ions. The LOD of the chemosensing probe for Sn^{2+} was calculated to be 0.115 μM, which is less than the WHO permissible amount of Sn^{2+} in drinking water. We further demonstrated that **4CBS** was utilized as a chemosensing probe to detect trace amounts of Sn^{2+} in human living cells and zebrafish. In contrast, the chemosensing probe **4CBS** detects Sn^{2+} in live cells, showing distinct fluorescence emission, which helps to differentiate human cancer cells from normal live cells.

ASSOCIATED CONTENT

Supporting Information

The Supporting Information is available free of charge at https://pubs.acs.org/doi/10.1021/acs.analchem.0c03196.

Synthetic procedures, spectral data, solvatochromic studies of the ligand **4CBS**, Job's plot, proposed optimized geometries of **4CBS** and its Sn^{2+} complex, and cell viability assay and bioimaging of **4CBS** (PDF)

https://dx.doi.org/10.1021/acs.analchem.0c03196
Anal. Chem. XXXX, XXX, XXX−XXX

AUTHOR INFORMATION

Corresponding Author

Dong Jin Yoo − *Department of Life Sciences, College of Natural Sciences and Department of Energy Storage/Conversion Engineering of Graduate School, and Hydrogen and Fuel Cell Research Center, Jeonbuk National University, Jeonju-si, Jeollabuk-do 54896, Republic of Korea;* orcid.org/0000-0002-5707-3361; Email: djyoo@jbnu.ac.kr

Authors

Palanisamy Ravichandiran − *Department of Life Sciences, College of Natural Sciences, Jeonbuk National University, Jeonju-si, Jeollabuk-do 54896, Republic of Korea;* orcid.org/0000-0001-5827-8230

Vignesh Krishnamoorthi Kaliannagounder − *Department of Bionanotechnology and Bioconvergence Engineering, Graduate School and Department of Bionanosystem Engineering, Graduate School, Jeonbuk National University, Jeonju-si, Jeollabuk-do 54896, Republic of Korea*

Antony Paulraj Bella − *PG and Research Department of Chemistry, Bishop Heber College, Tiruchirappalli, Tamil Nadu 620017, India*

Anna Boguszewska-Czubara − *Department of Medical Chemistry, Medical University of Lublin, Lublin 20-093, Poland*

Maciej Masłyk − *Department of Molecular Biology, Faculty of Biotechnology and Environmental Sciences, The John Paul II Catholic University of Lublin, Lublin 20-708, Poland*

Cheol Sang Kim − *Department of Bionanotechnology and Bioconvergence Engineering, Graduate School and Mechanical Design Engineering, Jeonbuk National University, Jeonju-si, Jeollabuk-do 54896, Republic of Korea*

Chan Hee Park − *Department of Bionanotechnology and Bioconvergence Engineering, Graduate School and Mechanical Design Engineering, Jeonbuk National University, Jeonju-si, Jeollabuk-do 54896, Republic of Korea*

Princy Merlin Johnson − *PG and Research Department of Chemistry, Bishop Heber College, Tiruchirappalli, Tamil Nadu 620017, India;* orcid.org/0000-0002-4294-9121

Byung-Hyun Park − *Department of Biochemistry, Jeonbuk National University Medical School, Jeonju-si, Jeollabuk-do 54896, Republic of Korea*

Myung-Kwan Han − *Department of Microbiology, Jeonbuk National University Medical School, Jeonju-si, Jeollabuk-do 54896, Republic of Korea*

Ae Rhan Kim − *Department of Life Sciences, College of Natural Sciences and Department of Energy Storage/Conversion Engineering of Graduate School, and Hydrogen and Fuel Cell Research Center, Jeonbuk National University, Jeonju-si, Jeollabuk-do 54896, Republic of Korea*

Complete contact information is available at: https://pubs.acs.org/10.1021/acs.analchem.0c03196

Notes

The authors declare no competing financial interest.

ACKNOWLEDGMENTS

This work was supported by grants from the Medical Research Center Program (NRF-2017R1A5A2015061) through the National Research Foundation (NRF), which is funded by the Korean government (MSIP). This research was also funded by Korea Institute of Energy Technology Evaluation and Planning (KETEP) and the Ministry of Trade, Industry & Energy (MOTIE) of the Republic of Korea (no. 20184030202210).

REFERENCES

(1) Cheng, H.-B.; Li, Y.; Tang, B. Z.; Yoon, J. *Chem. Soc. Rev.* **2020**, *49*, 21−31.
(2) Shirbhate, M. E.; Kwon, S.; Song, A.; Kim, S.; Kim, D.; Huang, H.; Kim, Y.; Lee, H.; Kim, S.-J.; Baik, M.-H.; Yoon, J.; Kim, K. M. *J. Am. Chem. Soc.* **2020**, *142*, 4975−4979.
(3) Nguyen, V. N.; Yim, Y.; Kim, S.; Ryu, B.; Swamy, K. M. K.; Kim, G.; Kwon, N.; Kim, C. Y.; Park, S.; Yoon, J. *Angew. Chem., Int. Ed.* **2020**, *59*, 8957−8962.
(4) Gul, A.; Oguz, M.; Kursunlu, A. N.; Yilmaz, M. *Dyes Pigm.* **2020**, *176*, 108221.
(5) Nguyen, V.-N.; Heo, S.; Kim, S.; Swamy, K. M. K.; Ha, J.; Park, S.; Yoon, J. *Sens. Actuators, B* **2020**, *317*, 128213.
(6) Brown, D. R. *Brain Res. Bull.* **2001**, *55*, 165−173.
(7) Gaggelli, E.; Kozlowski, H.; Valensin, D.; Valensin, G. *Chem. Rev.* **2006**, *106*, 1995−2044.
(8) Zhang, P.; Chen, S.; Kang, Y.; Long, Y. *Spectrochim. Acta, Part A* **2012**, *99*, 347−352.
(9) Heo, G.; Manivannan, R.; Kim, H.; Kim, M. J.; Min, K. S.; Son, Y.-A. *Sens. Actuators, B* **2019**, *297*, 126723.
(10) Salem, J. K.; El Nahhal, I. M.; H. Shurrab, M. *Int. J. Environ. Anal. Chem.* **2020**, 1−11.
(11) Lan, H.; Wen, Y.; Shi, Y.; Liu, K.; Mao, Y.; Yi, T. *Analyst* **2014**, *139*, 5223−5229.
(12) Wang, J.; Lv, M.; Wang, Z.; Zhou, M.; Gu, C.; Guo, C. *J. Photochem. Photobiol., A* **2015**, *309*, 37−46.
(13) Wei, S.; Zheng, C.; Liu, G.; Chen, B.; Pu, S. *J. Photochem. Photobiol., A* **2015**, *307*−*308*, 48−53.
(14) Adhikari, S.; Ghosh, A.; Guria, S.; Sahana, A. *RSC Adv.* **2016**, *6*, 39657−39662.
(15) Rüdel, H. *Ecotoxicol. Environ. Saf.* **2003**, *56*, 180−189.
(16) Capacho-Delgado, L.; Manning, D. C. *Spectrochim. Acta* **1966**, *22*, 1505−1513.
(17) Caldorin, R.; Menegário, A. A. *Microchim. Acta* **2007**, *157*, 201−207.
(18) Dongare, P. R.; Gore, A. H.; Ajalkar, B. D. *Inorg. Chim. Acta* **2020**, *502*, 119372.
(19) Mino, Y. *J. Health Sci.* **2006**, *52*, 67−72.
(20) Arvand, M.; Moghimi, A. M.; Afshari, A.; Mahmoodi, N. *Anal. Chim. Acta* **2006**, *579*, 102−108.
(21) Yoon, J.; Kim, S. K.; Singh, N. J.; Kim, K. S. *Chem. Soc. Rev.* **2006**, *35*, 355−360.
(22) Das, A. K.; Goswami, S. *Sens. Actuators, B* **2017**, *245*, 1062−1125.
(23) Guang, Y. S.; Ren, X.; Zhao, S.; Yan, Q. Z.; Zhao, G.; Xu, Y. H. *J. Environ. Sci. Health, Part A: Toxic/Hazard. Subst. Environ. Eng.* **2018**, *53*, 555−560.
(24) Peng, X.; Wu, Y.; Fan, J.; Tian, M.; Han, K. *J. Org. Chem.* **2005**, *70*, 10524−10531.
(25) Janeczko, M.; Demchuk, O. M.; Strzelecka, D.; Kubiński, K.; Masłyk, M. *Eur. J. Med. Chem.* **2016**, *124*, 1019−1025.
(26) Ravichandiran, P.; Subramaniyan, S. A.; Kim, S.-Y.; Kim, J.-S.; Park, B.-H.; Shim, K. S.; Yoo, D. J. *ChemMedChem* **2019**, *14*, 532−544.
(27) Ravichandiran, P.; Jegan, A.; Premnath, D.; Periasamy, V. S.; Muthusubramanian, S.; Vasanthkumar, S. *Bioorg. Chem.* **2014**, *53*, 24−36.
(28) Ravichandiran, P.; Masłyk, M.; Sheet, S.; Janeczko, M.; Premnath, D.; Kim, A. R.; Park, B. H.; Han, M. K.; Yoo, D. J. *ChemistryOpen* **2019**, *8*, 589−600.
(29) Bhasin, A. K. K.; Chauhan, P.; Chaudhary, S. *Sens. Actuators, B* **2019**, *294*, 116−122.

(30) Jonaghani, M. Z.; Zali-Boeini, H.; Taheri, R.; Rudbari, H. A.; Askari, B. *RSC Adv.* **2016**, *6*, 34940−34945.
(31) Qu, S.; Zheng, C.; Liao, G.; Fan, C.; Liu, G.; Pu, S. *RSC Adv.* **2017**, *7*, 9833−9839.
(32) Singh, G.; Diksha; Singh, A.; Sanchita; Sharma, G.; Shilpy; Pawan; Espinosa-Ruíz, C.; Esteban, M. A. *New J. Chem.* **2020**, *44*, 6238−6250.
(33) Gao, P.; Xie, Z.; Zheng, M. *Sens. Actuators, B* **2020**, *319*, 128265.
(34) Barrère, F.; Mahmood, T. A.; de Groot, K.; van Blitterswijk, C. A. *Mater. Sci. Eng., R* **2008**, *59*, 38−71.
(35) Yan, X.; Le, X. C. *Sci. China: Chem.* **2019**, *62*, 887−888.
(36) Faraz, M.; Abbasi, A.; Naqvi, F. K.; Khare, N.; Prasad, R.; Barman, I.; Pandey, R. *Sens. Actuators, B* **2018**, *269*, 195−202.
(37) Ravichandiran, P.; Subramaniyan, S. A.; Bella, A. P.; Johnson, P. M.; Kim, A. R.; Shim, K. S.; Yoo, D. J. *Anal. Chem.* **2019**, *91*, 10095−10101.
(38) Ravichandiran, P.; Boguszewska-Czubara, A.; Masłyk, M.; Bella, A. P.; Subramaniyan, S. A.; Johnson, P. M.; Shim, K. S.; Kim, H. G.; Yoo, D. J. *ACS Sustainable Chem. Eng.* **2019**, *7*, 17210−17219.
(39) Ravichandiran, P.; Prabakaran, D. S.; Bella, A. P.; Boguszewska-Czubara, A.; Masłyk, M.; Dineshkumar, K.; Johnson, P. M.; Park, B.-H.; Han, M.-K.; Kim, H. G.; Yoo, D. J. *ACS Sustainable Chem. Eng.* **2020**, *8*, 10947−10958.
(40) An Kim, P.; Lee, H.; So, H.; Kim, C. *Inorg. Chim. Acta* **2020**, *505*, 119502.
(41) Mohammadi, A.; Ghasemi, Z. *Spectrochim. Acta, Part A* **2020**, *228*, 117730.
(42) Koyappayil, A.; Kim, H. T.; Lee, M.-H. *Sens. Actuators, B* **2021**, *327*, 128887.
(43) Akiba, N.; Saitoh, N.; Kuroki, K. *J. Forensic Sci.* **2007**, *52*, 1103−1106.
(44) Comstock, M. J.; Comstock, M. J. In *Fluorescent Chemosensors for Ion and Molecule Recognition*; Comstock, M. J., Ed.; American Chemical Society, 1993; pp i−vi.
(45) Su, P.; Zhu, Z.; Wang, J.; Cheng, B.; Wu, W.; Iqbal, K.; Tang, Y. *Sens. Actuators, B* **2018**, *273*, 93−100.
(46) Ünal, U.; Somer, G. *Turk. J. Chem.* **2011**, *35*, 73−85.
(47) Pearson, R. G. *J. Am. Chem. Soc.* **1963**, *85*, 3533−3539.
(48) Bhuvanesh, N.; Suresh, S.; Velmurugan, K.; Thamilselvan, A.; Nandhakumar, R. *J. Photochem. Photobiol., A* **2020**, *386*, 112103.

https://dx.doi.org/10.1021/acs.analchem.0c03196
Anal. Chem. XXXX, XXX, XXX−XXX